Applied Mathematics & Information Sciences

Volume 10
Issue 5 *Sep. 2016*

Article 4

9-1-2016

A New Numerical Approach for the Solutions of Partial Differential Equations in Three-Dimensional Space

Brajesh Kumar Singh
Department of Applied Mathematics, School of Allied Sciences, Babasaheb Bhimrao Ambedkar University, Lucknow, Uttar Pradesh 226025, India, carlo.bianca@lps.ens.fr

Carlo Bianca
Laboratoire de Physique Statistique, Ecole Normale Sup´erieure, PSL Research University; Universit´e Paris Diderot Sorbonne Paris- Cit´e; Sorbonne Universit´es UPMC Univ Paris 06; CNRS; 24 rue Lhomond, 75005 Paris, France, carlo.bianca@lps.ens.fr

Applied Mathematics & Information Sciences
An International Journal

http://dx.doi.org/10.18576/amis/100504

A New Numerical Approach for the Solutions of Partial Differential Equations in Three-Dimensional Space

Brajesh Kumar Singh[1] *and Carlo Bianca*[2,*]

[1] Department of Applied Mathematics, School of Allied Sciences, Babasaheb Bhimrao Ambedkar University, Lucknow, Uttar Pradesh 226025, India
[2] Laboratoire de Physique Statistique, Ecole Normale Supérieure, PSL Research University; Université Paris Diderot Sorbonne Paris-Cité; Sorbonne Universités UPMC Univ Paris 06; CNRS; 24 rue Lhomond, 75005 Paris, France

Received: 10 Jan. 2016, Revised: 18 Apr. 2016, Accepted: 27 Apr. 2016
Published online: 1 Sep. 2016

Abstract: This paper deals with the numerical computation of the solutions of nonlinear partial differential equations in three-dimensional space subjected to boundary and initial conditions. Specifically, the modified cubic B-spline differential quadrature method is proposed where the cubic B-splines are employed as a set of basis functions in the differential quadrature method. The method transforms the three-dimensional nonlinear partial differential equation into a system of ordinary differential equations which is solved by considering an optimal five stage and fourth-order strong stability preserving Runge-Kutta scheme. The stability region of the numerical method is investigated and the accuracy and efficiency of the method are shown by means of three test problems: the three-dimensional space telegraph equation, the Van der Pol nonlinear wave equation and the dissipative wave equation. The results show that the numerical solution is in good agreement with the exact solution. Finally the comparison with the numerical solution obtained with some numerical methods proposed in the pertinent literature is performed.

Keywords: 3D nonlinear wave equation; modified cubic B-spline differential quadrature method; SSP-RK54 scheme, Thomas algorithm

1 Introduction

The development of numerical methods for the simulation of mathematical models has gained much attention considering that recently the power of the computers sciences has been increased. Various numerical methods have been proposed for obtaining numerical solutions of partial differential equations, see, among others, [1,2,3,4,5,6]. A highly accurate non-polynomial tension spline scheme for one-dimensional wave equation has been developed in [7] and applied to the one-dimensional wave equation. The numerical solution of the one-dimensional hyperbolic telegraph equation by using cubic B-spline collocation method has been obtained in [8]; numerical solutions of the multi-dimensional telegraphic has been investigated in [4]. Singh and Lin [9] have proposed a high order variable mesh off-step discretization scheme for the one-dimensional nonlinear hyperbolic equation; the reader interested to numerical methods for linear and nonlinear hyperbolic partial differential equations in three-dimensional space is referred to papers [4,10,11,12,13,14,15] and references cited therein. Recently in [5] an element-free Galerkin scheme has been proposed for the solution of the three-dimensional wave equation, and in [16] a element-free Galerkin method and a meshless local Petrov-Galerkin method have been proposed for the three-space-dimensional nonlinear wave equation.

The differential quadrature method (DQM) dates back to Bellman et al. [17,18]. In DQM the derivative of a function is approximated by introducing the weighted sum of the function values at certain discrete points. After the seminal paper of Bellman, various test functions have been proposed, among others, spline functions, sinc function, Lagrange interpolation polynomials, radial basis functions, see [19,20,21,22,23,24] and the references cited therein. In particular Shu and Richards [25] have developed one of the most generalized approach to solve the incompressible Navier-Stokes equation.

Recently, Arora and Singh [26] have proposed a *modified cubic B-spline differential quadrature method*

* Corresponding author e-mail: carlo.bianca@lps.ens.fr

(MCB-DQM) for the numerical computation of the solution of the one-dimensional Burger equation. The MCB-DQM has been further generalized for the computational modeling of partial differential equations in two-dimensional space [27] (the reader is referred also to papers [28,29]).

This paper is devoted to the development of a new MCB-DQM for the numerical simulation of the following partial differential equation in three-dimensional space:

$$\frac{\partial^2 u}{\partial t^2} + \alpha \frac{\partial u}{\partial t} + \beta u = \nabla^2 u + \delta g(u) \frac{\partial u}{\partial t} + f(x,y,z,t), \quad (1)$$

subject to the following initial condition (ICs):

$$\begin{cases} u(x,y,z,0) = \psi_1(x,y,z), & (x,y,z) \in \Omega \\ \frac{\partial u}{\partial t}(x,y,z,0) = \psi_2(x,y,z), & (x,y,z) \in \Omega \end{cases} \quad (2)$$

and to the Dirichlet boundary condition (BCs):

$$u(x,y,z,t) = \xi(x,y,z), \quad (x,y,z) \in \partial\Omega, t > 0, \quad (3)$$

where $\nabla^2 \equiv \frac{\partial^2}{\partial x^2} + \frac{\partial^2}{\partial y^2} + \frac{\partial^2}{\partial z^2}$, $\Omega = \{(x,y,z) : 0 \leq x,y,z \leq 1\}$ is the computational domain and $\partial\Omega$ is the boundary of Ω. The function $u(x,y,z,t)$ is the unknown function whereas f, ψ_1, ψ_2 and ξ are known functions.

The MCB-DQM is used for computing the spatial derivatives. Accordingly the partial differential equation is transformed into a system of first-order ordinary differential equations which is then solved by using the SSP-RK54 scheme [28,29]. The stability region of the numerical method is investigated within the paper and the accuracy and efficiency of the method are studied by means of three test problems: the three-dimensional space telegraph equation, the Van der Pol nonlinear wave equation and the dissipative wave equation. The results show that the numerical solution is in good agreement with the exact solution. Finally the comparison with the numerical solution obtained with some numerical methods proposed in the pertinent literature is performed. Specifically the Root Mean Square (RMS) error norm in the MCB-DQM solutions is compared with the error obtained with the MLPG [16] and the EFP [16].

The paper is organized into five more sections, which follow this introduction. Specifically Section 2 deals with the description of the modified cubic B-spline differential quadrature method. Section 3 is devoted to the procedure for the implementation of method for the problem (1) with the initial conditions (2) and boundary conditions (3). The stability analysis of the MCB-DQM is discussed in Section 4. Section 5 is concerned with three test problems with the main aim to establish the accuracy of the proposed method in terms of the RMS error norm. Finally Section 6 concludes the paper with reference to critical analysis and research perspectives.

2 The modified cubic B-spline differential quadrature method

This section deals with the description of the MCB-DQM [26,27,30,31] for the partial differential equation in three-dimensional space (1). Let $\mathbb{D}$ be the following domain:

$$\mathbb{D} = \{(x,y,z) \in \mathbb{R}^3 : a \leq x \leq b, c \leq y \leq d, \ell \leq z \leq m\}$$

which is uniformly partitioned in each direction with the following knots:

$$a = x_1 < x_2 < \ldots < x_i < \ldots < x_{N_x - 1} < x_{N_x} = b,$$

$$c = y_1 < y_2 < \ldots < y_j < \ldots < y_{N_y - 1} < y_{N_y} = d,$$

$$\ell = z_1 < z_2 < \ldots < z_k < \ldots < z_{N_z - 1} < z_{N_z} = m,$$

where

$$h_x = \frac{b-a}{N_x - 1}, \quad h_y = \frac{d-c}{N_y - 1}, \quad h_z = \frac{m-\ell}{N_z - 1},$$

is the discretization step in the x, y and z directions, respectively. Let (x_i, y_j, z_k) be the generic grid point and

$$u_{ijk} \equiv u_{ijk}(t) \equiv u(x_i, y_j, z_k, t),$$

for $i \in \Delta_x = \{1,2,\ldots,N_x\}$, $j \in \Delta_y = \{1,2,\ldots,N_y\}$ and $k \in \Delta_z = \{1,2,\ldots,N_z\}$.
The rth-order partial derivatives of $u(x,y,z,t)$, for $r \in \{1,2\}$, with respect to x, y, z and evaluated in the grid point (x_i, y_j, z_k) are approximated as follows:

$$\begin{aligned} \frac{\partial^r u}{\partial x^r}(x_i,y_j,z_k) &= \sum_{p=1}^{N_x} a_{ip}^{(r)} u_{pjk}, & i \in \Delta_x, \\ \frac{\partial^r u}{\partial y^r}(x_i,y_j,z_k) &= \sum_{p=1}^{N_y} b_{jp}^{(r)} u_{ipk}, & j \in \Delta_y, \\ \frac{\partial^r u}{\partial z^r}(x_i,y_j,z_k) &= \sum_{p=1}^{N_z} c_{kp}^{(r)} u_{ijp}, & k \in \Delta_z, \end{aligned} \quad (4)$$

where $a_{ip}^{(r)}$, $b_{jp}^{(r)}$ and $c_{kp}^{(r)}$, called the weighting functions of the rth-order partial derivative, are the unknown time dependent quantities to be determined.
The cubic B-splines function $\varphi_i = \varphi_i(x)$, in the x direction and at the knots, reads:

$$\varphi_i = \frac{1}{h_x^3} \begin{cases} (x - x_{i-2})^3 & x \in [x_{i-2}, x_{i-1}) \\ (x - x_{i-2})^3 - 4(x - x_{i-1})^3 & x \in [x_{i-1}, x_i) \\ (x_{i+2} - x)^3 - 4(x_{i+1} - x)^3 & x \in [x_i, x_{i+1}) \\ (x_{i+2} - x)^3 & x \in [x_{i+1}, x_{i+2}) \\ 0 & \text{otherwise} \end{cases} \quad (5)$$

The set $\{\varphi_0, \varphi_1, \varphi_2, \ldots, \varphi_{N_x}, \varphi_{N_x+1}\}$ is a basis over the set $[a,b]$. The values of φ_i and its first and second derivatives in the grid point x_j, denoted by $\varphi_{ij} := \varphi_i(x_j)$, $\varphi'_{ij} := \varphi'_i(x_j)$ and $\varphi''_{ij} := \varphi''_i(x_j)$, respectively, read:

$$\varphi_{ij} = \begin{cases} 4, & \text{if } i-j=0 \\ 1, & \text{if } i-j=\pm 1 \\ 0, & \text{otherwise} \end{cases} \quad (6)$$

$$\varphi'_{ij} = \begin{cases} 3/h_x, & \text{if } i-j=1 \\ -3/h_x, & \text{if } i-j=-1 \\ 0, & \text{otherwise} \end{cases} \quad (7)$$

$$\varphi''_{ij} = \begin{cases} -12/h_x^2, & \text{if } i-j=0 \\ 6/h_x^2, & \text{if } i-j=\pm 1 \\ 0 & \text{otherwise} \end{cases} \quad (8)$$

The modified cubic B-splines basis functions are obtained by modifying the cubic B-spline basis functions (5) as follows [26]:

$$\begin{cases} \phi_1(x) = \varphi_1(x) + 2\varphi_0(x) \\ \phi_2(x) = \varphi_2(x) - \varphi_0(x) \\ \vdots \\ \phi_j(x) = \varphi_j(x), \text{ for } j = 3,4,\ldots,N_x-2 \\ \vdots \\ \phi_{N_x-1}(x) = \varphi_{N_x-1}(x) - \varphi_{N_x+1}(x) \\ \phi_{N_x}(x) = \varphi_{N_x}(x) + 2\varphi_{N_x+1}(x) \end{cases} \quad (9)$$

The set $\{\phi_1, \phi_2, \ldots, \phi_{N_x}\}$ is a basis over the set $[a,b]$. Analogously procedure is followed for the y and z directions.

2.1 Computation of the weighting coefficients

In order to compute the weighting coefficients $a_{ip}^{(1)}$ of Eq. (4), we use the modified cubic B-spline $\phi_p(x)$, $p \in \Delta_x$. Let $\phi'_{pi} := \phi'_p(x_i)$ and $\phi_{p\ell} := \phi_p(x_\ell)$. Accordingly the approximation of the first-order derivative is obtained as follows:

$$\phi'_{pi} = \sum_{\ell=1}^{N_x} a_{i\ell}^{(1)} \phi_{p\ell}, \qquad p,i \in \Delta_x. \quad (10)$$

Setting $\Phi = [\phi_{p\ell}]$, $A = [a_{i\ell}^{(1)}]$ (the unknown weighting coefficient matrix), and $\Phi' = [\phi'_{pi}]$, then Eq. (10) can be re-written as the following system of linear equations:

$$\Phi A^T = \Phi'. \quad (11)$$

The coefficient matrix Φ of order N_x can be obtained from (6) and (9):

$$\Phi = \begin{bmatrix} 6 & 1 & & & & & \\ 0 & 4 & 1 & & & & \\ & 1 & 4 & 1 & & & \\ & & \ddots & \ddots & \ddots & & \\ & & & 1 & 4 & 1 & \\ & & & & 1 & 4 & 0 \\ & & & & & 1 & 6 \end{bmatrix}$$

and in particular the columns of the matrix Φ' read:

$$\Phi'[1] = \begin{bmatrix} -6/h_x \\ 6/h_x \\ 0 \\ \vdots \\ 0 \\ 0 \end{bmatrix}, \Phi'[2] = \begin{bmatrix} -3/h_x \\ 0 \\ 3/h_x \\ 0 \\ \vdots \\ 0 \end{bmatrix}, \ldots,$$

$$\Phi'[N_x-1] = \begin{bmatrix} 0 \\ \vdots \\ 0 \\ -3/h_x \\ 0 \\ 3/h_x \end{bmatrix}, \text{ and } \Phi'[N_x] = \begin{bmatrix} 0 \\ \vdots \\ 0 \\ -6/h_x \\ 6/h_x \end{bmatrix}.$$

It is worth stressing that the cubic B-splines are modified in order to have a diagonally dominant coefficient matrix Φ, see Eq. (11). The system (11) is thus solved by employing the Thomas Algorithm [32].

Similarly, the weighting coefficients $b_{ip}^{(1)}$ and $c_{ip}^{(1)}$ can be computed considering the grid in the y and z directions.

The weighting coefficients $a_{ip}^{(r)}$, $b_{ip}^{(r)}$ and $c_{ip}^{(r)}$, for $r \geq 2$, can be computed by using the following Shu's recursive formulae [21]:

$$\begin{cases} a_{ij}^{(r)} = r\left(a_{ij}^{(1)} a_{ii}^{(r-1)} - \dfrac{a_{ij}^{(r-1)}}{x_i - x_j}\right), i \neq j : i,j \in \Delta_x, \\ a_{ii}^{(r)} = -\displaystyle\sum_{i=1, i\neq j}^{N_x} a_{ij}^{(r)}, i = j : i,j \in \Delta_x. \\ b_{ij}^{(r)} = r\left(b_{ij}^{(1)} b_{ii}^{(r-1)} - \dfrac{b_{ij}^{(r-1)}}{y_i - y_j}\right), i \neq j : i,j \in \Delta_y \\ b_{ii}^{(r)} = -\displaystyle\sum_{i=1, i\neq j}^{N_y} b_{ij}^{(r)}, i = j : i,j \in \Delta_y. \\ c_{ij}^{(r)} = r\left(c_{ij}^{(1)} c_{ii}^{(r-1)} - \dfrac{c_{ij}^{(r-1)}}{z_i - z_j}\right), i \neq j : i,j \in \Delta_z \\ c_{ii}^{(r)} = -\displaystyle\sum_{i=1, i\neq j}^{N_z} c_{ij}^{(r)}, i = j : i,j \in \Delta_z. \end{cases} \quad (12)$$

3 The numerical scheme of MCB-DQM

Setting $\frac{\partial u}{\partial t} = v$ and thus $\frac{\partial^2 u}{\partial t^2} = \frac{\partial v}{\partial t}$, and $f(x_i, y_j, z_k, t) = f_{ijk}$, the numerical scheme transforms

Eqs. (1)-(2) into the following problem:

$$\begin{cases} \dfrac{du_{ijk}}{dt} = v_{ijk} \\ \dfrac{dv_{ijk}}{dt} = \sum_{p=1}^{N_x} a_{ip}^{(2)} u_{pjk} + \sum_{p=1}^{N_y} b_{jp}^{(2)} u_{ipk} + \sum_{p=1}^{N_z} c_{kp}^{(2)} u_{ijp} + K_{ijk} \\ u_{ijk}(t=0) = \psi_1(x_i, y_j, z_k), \\ v_{ijk}(t=0) = \psi_2(x_i, y_j, z_k), \end{cases} \tag{13}$$

where $i \in \Delta_x, j \in \Delta_y, k \in \Delta_z$ and

$$K_{ijk} = (\delta g(u_{ijk}) - \alpha) v_{ijk} - \beta u_{ijk} + f_{ijk}.$$

Bearing the boundary condition (3) in mind, Eq. (13) is rewritten as follows:

$$\begin{cases} \dfrac{du_{ijk}}{dt} = v_{ijk} \\ \dfrac{dv_{ijk}}{dt} = \sum_{p=2}^{N_x-1} a_{ip}^{(2)} u_{pjk} + \sum_{p=2}^{N_y-1} b_{jp}^{(2)} u_{ipk} + \sum_{p=2}^{N_z-1} c_{kp}^{(2)} u_{ijp} + F_{ijk} \\ u_{ijk}(t=0) = \psi_1(x_i, y_j, z_k), \\ v_{ijk}(t=0) = \psi_2(x_i, y_j, z_k), \end{cases} \tag{14}$$

where $2 \le i \le N_x - 1, 2 \le j \le N_y - 1, 2 \le k \le N_z - 1$ and

$$\begin{aligned} F_{ijk} = K_{ijk} + a_{i1}^{(2)} u_{1jk} + a_{iN_x}^{(2)} u_{N_x jk} + b_{j1}^{(2)} u_{i1k} \\ + b_{jN_y}^{(2)} u_{iN_y k} + c_{k1}^{(2)} u_{ij1} + c_{k,N_z}^{(2)} u_{ijN_z}. \end{aligned} \tag{15}$$

Various numerical schemes have been proposed to solve initial value problems, among others, the SSP-RK scheme allows low storage and large region of absolute property [29,28]. In particular in what follows we consider the following SSP-RK54 scheme which is strongly stable for nonlinear hyperbolic differential equations:

$$\begin{aligned} u^{(1)} &= u^m + 0.391752226571890 \triangle t L(u^m) \\ u^{(2)} &= 0.444370493651235 v^m + 0.555629506348765 u^{(1)} \\ &\quad + 0.368410593050371 \triangle t L(u^{(1)}) \\ u^{(3)} &= 0.620101851488403 u^m + 0.379898148511597 u^{(2)} \\ &\quad + 0.251891774271694 \triangle t L(u^{(2)}) \\ u^{(4)} &= 0.178079954393132 u^m + 0.821920045606868 u^{(3)} \\ &\quad + 0.544974750228521 \triangle t L(u^{(3)}) \\ u^{m+1} &= 0.517231671970585 u^{(2)} + 0.096059710526147 u^{(3)} \\ &\quad + 0.063692468666290 \triangle t L(u^{(3)}) + 0.386708617503269 u^{(4)} \\ &\quad + 0.226007483236906 \triangle t L(u^{(4)}) \end{aligned}$$

4 Stability Analysis

In what follows, we assume $\alpha > \delta g$. The system (14) can be rewritten in compact form as follows:

$$\frac{dU}{dt} = AU + G,$$

or

$$\frac{d}{dt}\begin{bmatrix} u \\ v \end{bmatrix} = \begin{bmatrix} O & I \\ B & (\delta g - \alpha) I \end{bmatrix} \begin{bmatrix} u \\ v \end{bmatrix} + \begin{bmatrix} O_1 \\ F \end{bmatrix} \tag{16}$$

where

$a)$ O and O_1 are null matrices;

$b)$ I is the identity matrix of order $(N_x - 2)(N_y - 2)(N_z - 2)$;

$c)$ $U = (u, v)^T$ the vector solution at the grid points: $u = (u_{222}, u_{223}, \ldots, u_{22(N_z-1)}, u_{232}, u_{233}, \ldots, u_{23(N_z-1)}, \ldots, u_{(N_x-1)(N_y-1)3}, \ldots, u_{N_x-1)(N_y-1)(N_z-1)})$. $v = (v_{222}, v_{223}, \ldots, v_{22(N_z-1)}, v_{232}, v_{233}, \ldots, v_{23(N_z-1)}, \ldots, v_{(N_x-1)(N_y-1)3}, \ldots, v_{N_x-1)(N_y-1)(N_z-1)})$.

$d)$ $F = (F_{222}, F_{223}, \ldots, F_{22(N_z-1)}, F_{232}, F_{233}, \ldots, F_{23(N_z-1)}, \ldots, F_{(N_x-1)(N_y-1)3}, \ldots, F_{N_x-1)(N_y-1)(N_z-1)})$, where F_{ijk} is defined in Eq. (15).

$e)$ $B = -\beta I + B_x + B_y + B_z$, where B_x, B_y and B_z are the following matrices (of order $(N_x - 2)$, $(N_y - 2)$, $(N_z - 2)$, respectively) of the weighting coefficients $a_{ij}^{(2)}$, $b_{ij}^{(2)}$ and $c_{ij}^{(2)}$:

$$B_x = \begin{bmatrix} a_{22}^{(2)} I_x & a_{23}^{(2)} I_x & \ldots & a_{2(N_x-1)}^{(2)} I_x \\ a_{32}^{(2)} I_x & a_{33}^{(2)} I_x & \ldots & a_{3(N_x-1)}^{(2)} I_x \\ \vdots & \vdots & \ddots & \vdots \\ a_{(N_x-1)2}^{(2)} I_x & a_{(N_x-2)3}^{(2)} I_x & \ldots & a_{(N_x-1)(N_x-1)}^{(2)} I_x \end{bmatrix} \tag{17}$$

$$B_y = \begin{bmatrix} M_y & O_y & \ldots & O_y \\ O_y & M_y & \ldots & O_y \\ \vdots & \vdots & \ddots & \vdots \\ O_y & O_y & \ldots & M_y \end{bmatrix} \quad B_z = \begin{bmatrix} M_z & O_z & \ldots & O_z \\ O_z & M_z & \ldots & O_z \\ \vdots & \vdots & \ddots & \vdots \\ O_z & O_z & \ldots & M_z \end{bmatrix} \tag{18}$$

where

$$M_y = \begin{bmatrix} b_{22}^{(2)} I_z & b_{23}^{(2)} I_z & \ldots & b_{2(N_y-1)}^{(2)} I_z \\ b_{32}^{(2)} I_z & b_{33}^{(2)} I_z & \ldots & b_{3(M-1)}^{(2)} I_z \\ \vdots & \vdots & \ddots & \vdots \\ b_{(N_y-1)2}^{(2)} I_z & b_{(N_y-1)3}^{(2)} I_z & \ldots & b_{(N_y-1)(N_y-1)}^{(2)} I_z \end{bmatrix}$$

and

$$M_z = \begin{bmatrix} c_{22}^{(2)} & c_{23}^{(2)} & \ldots & c_{2(N_z-1)}^{(2)} \\ c_{32}^{(2)} & c_{33}^{(2)} & \ldots & c_{3(N_z-1)}^{(2)} \\ \vdots & \vdots & \ddots & \vdots \\ c_{(N_z-1)2}^{(2)} & c_{(N_z-1)3}^{(2)} & \ldots & c_{(N_z-1)(N_z-1)}^{(2)} \end{bmatrix}$$

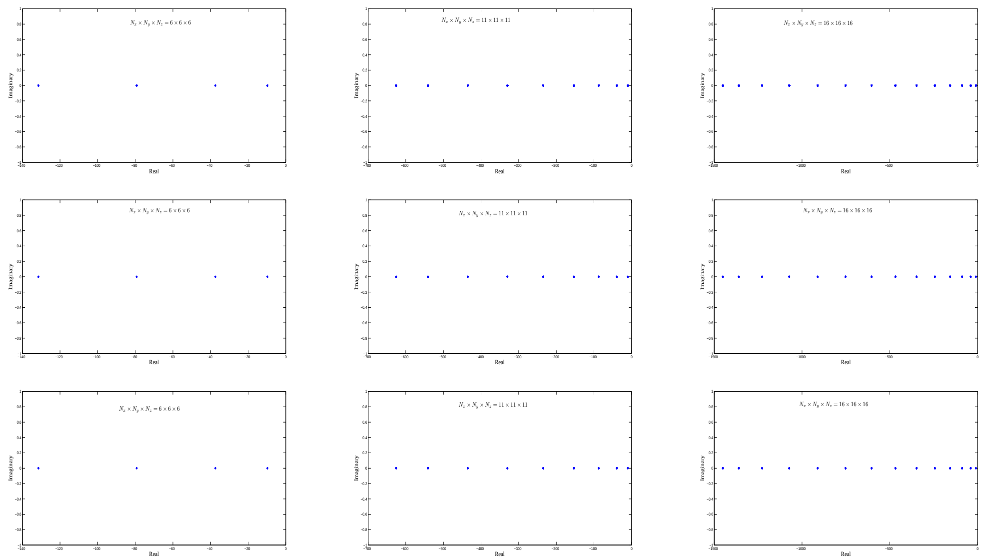

Fig. 1: Eigenvalues of B_x (first row), B_y (second row) and B_z (third row) for different values of the grid points.

where O_y and O_z are null matrices of order $(N_y-2)(N_z-2)$ and (N_z-2), respectively; I_x and I_z are the identity matrices of order $(N_y-2)(N_z-2)$ and (N_z-2), respectively.

The stability of the numerical scheme proposed for (1) depends on the stability of the system of ODEs defined in (16). If the system of ODEs (16) is unstable, then the numerical scheme for temporal discretization may not converge. Since the exact solution can be directly obtained by means of the eigenvalues method, the stability of (16) depends on the eigenvalues of the coefficient matrix A. Accordingly the system (16) is stable if the real part of each eigenvalue of A is zero or negative.

Let λ_A be an eigenvalue of A associated with the eigenvector $(X_1,X_2)^T$, where each component is a vector of order $(N_x-2)(N_y-2)(N_z-2)$. Then from Eq. (16) we have

$$A\begin{bmatrix} X_1 \\ X_2 \end{bmatrix} = \begin{bmatrix} O & I \\ B & (\delta g-\alpha)I \end{bmatrix}\begin{bmatrix} X_1 \\ X_2 \end{bmatrix} = \lambda_A \begin{bmatrix} X_1 \\ X_2 \end{bmatrix}, \tag{19}$$

which implies that

$$IX_2 = \lambda_A X_1, \tag{20}$$

and

$$BX_1 + (\delta g - \alpha)X_2 = \lambda_A X_2. \tag{21}$$

Simplifying Eq. (20) and Eq. (21), we get

$$BX_1 = \lambda_A(\lambda_A + \alpha - \delta g)X_1. \tag{22}$$

This shows that the eigenvalue λ_B of B is $\lambda_B = \lambda_A(\lambda_A + \alpha - \delta g)$. We now consider the matrix

$$B = -\beta I + B_x + B_y + B_z, \tag{23}$$

and we compute the eigenvalues of B_x, B_y and B_z for different grid points: $6\times 6\times 6$, $11\times 11\times 11$ and $16\times 16\times 16$. As Fig 1 shows, for different values of the grid points the computed eigenvalues of B_x, B_y and B_z are real negative numbers. Since $\beta > 0$, from Eq.(23) we have

$$Re(\lambda_B) \le 0 \quad \text{and} \quad Im(\lambda_B) = 0, \tag{24}$$

where $Re(z)$ and $Im(z)$ denote the real and the imaginary part of z, respectively. Let $\lambda_A = x + \imath y$, then

$$\begin{aligned} \lambda_B &= \lambda_A(\lambda_A + \alpha - \delta g) \\ &= x^2 - y^2 + (\alpha - \delta g)x + \imath(2x + (\alpha - \delta g))y. \end{aligned} \tag{25}$$

According to Eq. (24) and Eq. (25), we have

$$\begin{cases} x^2 - y^2 + (\alpha - \delta g)x < 0 \\ (2x + (\alpha - \delta g))y = 0 \end{cases} \tag{26}$$

The possible solutions of Eq.(26) are

1)If $y \neq 0$, then $x = -\frac{\alpha - \delta g}{2}$,
2)If $y = 0$, then $\left(x + \frac{(\alpha-\delta g)}{2}\right)^2 < \left(\frac{(\alpha-\delta g)}{2}\right)^2$.

The proposed scheme is thus stable if $\alpha > \delta g$.

5 Numerical experiments

This section is devoted to the accuracy analysis of the proposed numerical method. Specifically three test cases of (1) are taken into account. The accuracy and

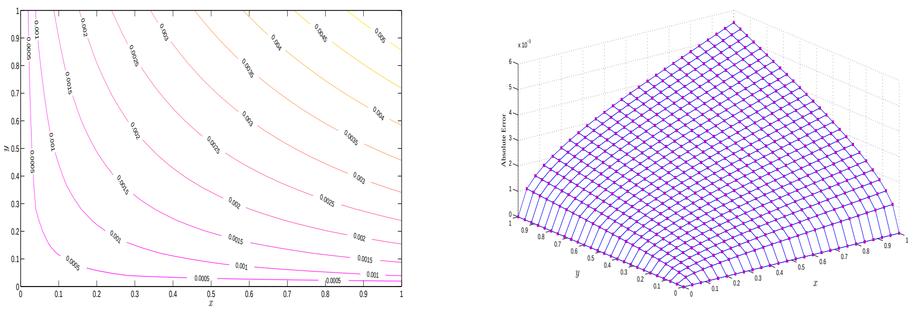

Fig. 2: The contour plot (left panel) and surface plot (right panel) of the absolute error in the three-dimensional telegraph equation of the Problem 1 for $z = 0.5$, $t = 1$, $h = 0.044$, $\triangle t = 0.01$.

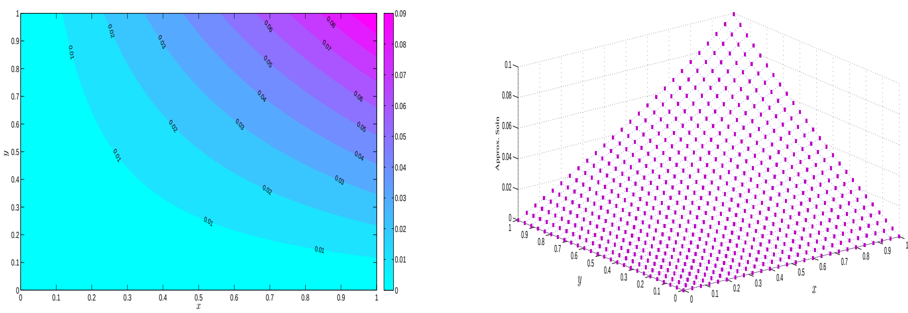

Fig. 3: The contour plot (left panel) and surface plot (right panel) of the numerical solution of the three-dimensional telegraph equation of the Problem 1 for $z = 0.5$, $t = 1$, $h = 0.04$, $\triangle t = 0.01$.

consistency of the method is performed by considering the following RMS error norm:

$$\mathrm{RMS} = \left(\frac{\sum_{i=1}^{N_x} \sum_{j=1}^{N_y} \sum_{k=1}^{N_z} \left| u_{ijk} - u^*_{ijk} \right|^2}{N_x N_y N_z} \right)^{\frac{1}{2}}$$

where u_{ijk} and u^*_{ijk} denote the numerical solution and the exact solution at (x_i, y_j, z_k), respectively.

Problem 1. The first test case deals with the three-dimensional *linear telegraph hyperbolic* equation [4,16], which corresponds to $\delta = 0$, $\alpha = \beta = 2$. We consider as exact solution of the equation (1)-(3) the following function:

$$u(x,y,z,t) = \sinh(x)\sinh(y)\sinh(z)e^{-2t}, (x,y,z) \in \Omega, t \geq 0,$$

with $\psi_1(x,y,z), \psi_2(x,y,z)$, $\xi(x,y,z,t)$, and $f(x,y,z,t)$ obtained accordingly.

The numerical solution for the problem 1 is obtained for $\triangle t = 0.01$ and grid size $11 \times 11 \times 11$. Table 1 summarizes the RMS error obtained with the MCB-DQM, the MLPG [16] and the EFP [16]. The Fig. 2 shows the RMS for the MCB-DQM solution for $z = 0.5$, grid size $26 \times 26 \times 26$ and at time $t = 1.0$; the Fig. 3 shows the MCB-DQM solution for $z = 0.5$, grid size $25 \times 25 \times 25$ and at time $t = 1.0$. The numerical solution is in good agreement with the exact solution.

Problem 2. The second test case deals with the *Van der Pol* nonlinear wave equation [16,4], which corresponds to $\alpha = \delta = \kappa, \beta = 0$ and $g(u) = u^2$. We consider as exact solution of the equation (1)-(3) the following function:

$$u(x,y,z,t) = \sin(x)\sin(y)\sin(z)e^{-\kappa t}, (x,y,z) \in \Omega, t \geq 0. \quad (27)$$

with $\psi_1(x,y,z)$, $\psi_2(x,y,z)$, $\xi(x,y,z,t)$ and $f(x,y,z,t)$ defined accordingly.

The numerical solution of the Problem 2 is obtained for $\kappa = 3$, $\triangle t = 0.01$ and grid size $11 \times 11 \times 11$. Table 2 summarizes the RMS error norm for the MCB-DQM, the MLPG [16] and the EFP [16]. The Fig. 4 shows the absolute error for the MCB-DQM solution for $z = 1.0$, grid size $25 \times 25 \times 25$ and at time $t = 1.0$. The contour plot and the surface plots of the MCB-DQM solution are depicted in Fig. 5 and in Fig. 6, respectively. The numerical solution is in good agreement with the exact solution.

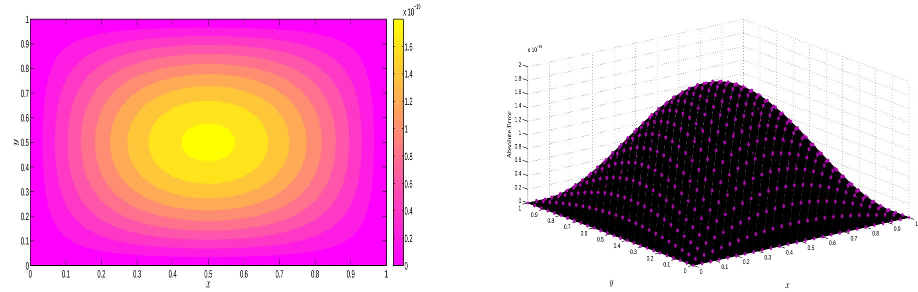

Fig. 4: The contour plot (left panel) and surface plot (right panel) of the absolute error in the three-dimensional nonlinear Van der Pol equation of the Problem 2 for $z = 1.0$, $t = 1$, $h = 0.04$, and $\triangle t = 0.01$.

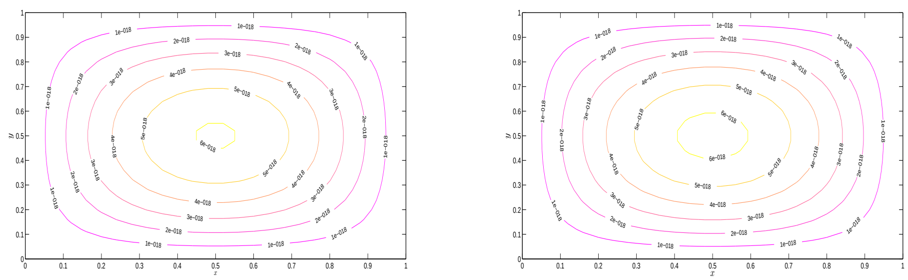

Fig. 5: The contour plot of the exact solution (left panel) and of the MCB-DQM solution (right panel) for the three-dimensional nonlinear Van der Pol equation of the Problem 2 for $z = 1.0$, $t = 1$, $h = 0.04$, $\triangle t = 0.01$.

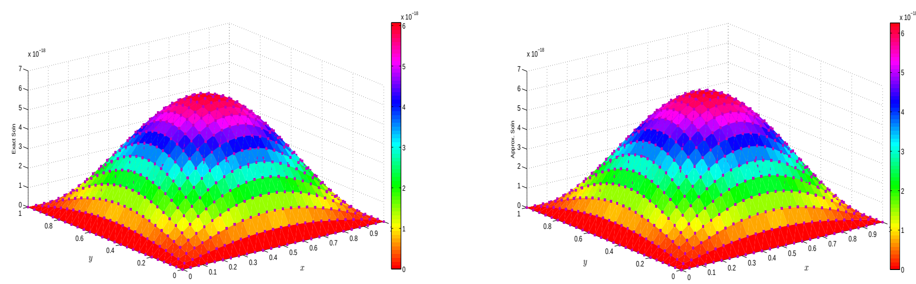

Fig. 6: The surface plot of the exact solution (left panel) and numerical solution (right panel) of the three-dimensional nonlinear Van der Pol equation of the Problem 2 for $z = 1$, $t = 1$, $h = 0.04$, $\triangle t = 0.01$.

Problem 3. The third test case is devoted to the three-dimensional nonlinear wave equation in *the dissipative form*, which corresponds to $\alpha = \beta = 0$, $\delta = -2$ and $g(u) = u$. We consider as exact solution of the equation (1)-(3) the following function:

$$u(x,y,z,t) = \sin(t)\prod_{x,y,z}\sin(\pi x), (x,y,z) \in \Omega, t \geq 0, \quad (28)$$

with $\psi_1(x,y,z)$, $\psi_2(x,y,z)$, $\xi(x,y,z,t)$ and $f(x,y,z,t)$ defined accordingly.

The numerical solution of the Problem 3 is obtained for $\triangle t = 0.01$ and grid size $11 \times 11 \times 11$. Table 3 summarizes the RMS error norm obtained with the MCB-DQM, the MLPG[16] and the EFP[16]. The Fig. 7 depicts the absolute error for the MCB-DQM solution for $z = 0.5$, grid size $25 \times 25 \times 25$ and at time $t = 1.0$. The contour plot and the surface plot of the MCB-DQM solution are shown in Fig. 8 and 9, respectively. The numerical solution is in good agreement with the exact solution.

6 Conclusions

The present paper is concerned with the definition of a new numerical method based on the MCB-DQM for the derivation of numerical solutions for partial differential equations in three-dimensional space. The main aim is to improve the accuracy of the numerical solutions, which relies on the strong and efficient implementation of the method. The large computational cost is the main drawback of almost all methods available in the literature

Table 1: The RMS error norm for the MCB-DQM, the MLPG [16] and the EFP [16] ($\triangle t = 0.01$ and grid size $11 \times 11 \times 11$) for the Problem 1.

t	MCB-DQM	MLPG[16]	EFP[16]	CPU time (seconds)
0.1	1.01409e-006	6.389040e-004	1.361376e-001	0.077
0.2	1.66777e-006	1.621007e-003	1.108673e-001	0.140
0.3	1.72678e-006	2.069397e-003	9.031794e-002	0.207
0.4	1.49946e-006	1.851491e-003	7.555177e-002	0.266
0.5	1.19699e-006	1.406413e-003	6.113317e-002	0.326
0.6	9.06725e-007	1.120239e-003	5.076050e-002	0.385
0.7	7.06686e-007	8.762877e-004	4.276296e-002	0.444
0.8	5.57041e-007	5.762842e-004	3.416178e-002	0.505
0.9	4.76172e-007	7.778958e-004	3.072394e-002	0.565
1.0	4.42082e-007	8.638225e-004	2.562088e-002	0.624

Table 2: The RMS error norm for the MCB-DQM, the MLPG [16] and the EFP [16] ($\triangle t = 0.01$ and grid size $11 \times 11 \times 11$) for the Problem 2

t	MCB-DQM	MLPG[16]	EFP[16]	CPU time (seconds)
0.1	5.67101e-006	2.777931e-003	1.653265e+000	0.140
0.2	9.70224e-006	8.477482e-003	1.005632e+000	0.250
0.3	1.23148e-005	1.352534e-002	9.786343e-001	0.370
0.4	1.51181e-005	1.583307e-002	7.456237e-001	0.490
0.5	1.82388e-005	1.550351e-002	6.213675e-001	0.610
0.6	2.22188e-005	1.367202e-002	4.354421e-001	0.730
0.7	2.57046e-005	1.052578e-002	1.345213e-001	0.851
0.8	2.86607e-005	6.216680e-003	9.973233e-002	0.971
0.9	3.11707e-005	5.280951e-003	7.132423e-002	1.091
1.0	3.32916e-005	2.276681e-003	6.124572e-002	1.211

Table 3: The RMS error norm for the MCB-DQM, the MLPG [16] and the EFP [16] ($\triangle t = 0.01$ and grid size $11 \times 11 \times 11$) for the Problem 3.

t	MCB-DQM	MLPG[16]	EFP[16]	CPU time (seconds)
0.1	2.90131e-007	8.903029e-005	1.435666e-003	0.140
0.2	1.25781e-006	9.910264e-005	3.867576e-003	0.240
0.3	2.94185e-006	1.590358e-004	5.033494e-003	0.360
0.4	5.34148e-006	3.776687e-004	7.655177e-003	0.480
0.5	8.77107e-006	4.781290e-004	9.119769e-003	0.612
0.6	1.35793e-005	6.416380e-004	1.034540e-002	0.732
0.7	2.02462e-005	8.809498e-004	3.279875e-002	0.852
0.8	2.91101e-005	9.279331e-004	5.233178e-002	0.972
0.9	4.03845e-005	1.059260e-004	6.072234e-002	1.082
1.0	5.41878e-005	1.529316e-003	7.545088e-002	1.202

for the solution of three-dimensional partial differential equations.

The analysis of the accuracy and effectiveness of the method is performed by considering three test cases: the three-dimensional *linear telegraphic equation, the Van der Pol type nonlinear wave equation and the dissipative nonlinear wave equation*. The analysis of the root mean square error shows that the MCB-DQM solutions are more accurate of the numerical solutions obtained with the existing methods of the pertinent literature [16].

Research perspectives include the possibility to develop further refinements of the method proposed in the present paper for the derivation of numerical solutions for kinetic equations [33] and specifically for thermostatted

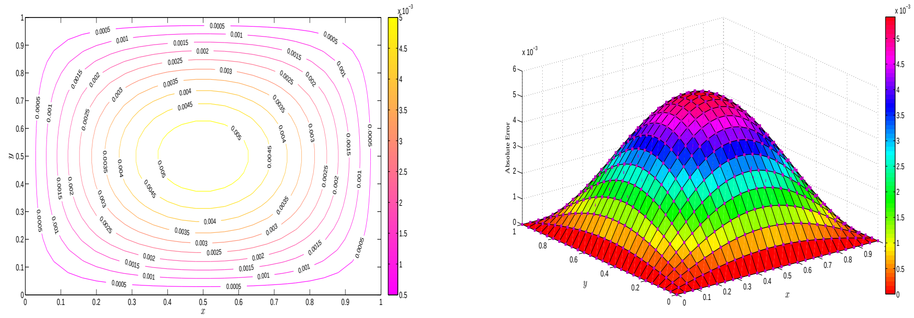

Fig. 7: The contour plot (left panel) and surface plot (right panel) of the absolute error in the three-dimensional nonlinear wave equation in dissipative form of the Problem 3 for $z = 0.5$, $t = 1$, $h = 0.04$, and $\triangle t = 0.01$.

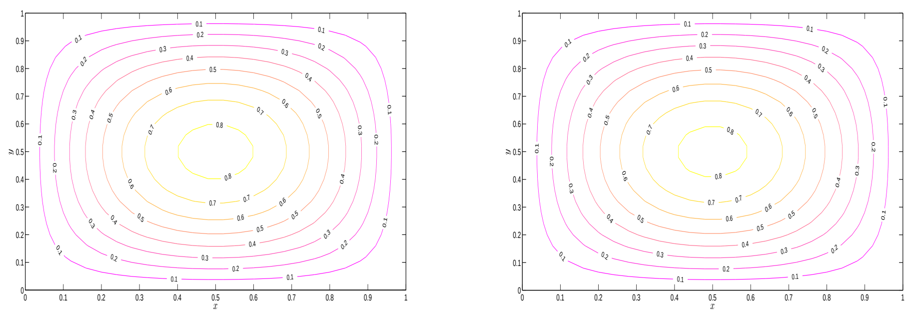

Fig. 8: The contour plot of the exact solution (left panel) and of the MCB-DQM solution (right panel) for the three-dimensional nonlinear wave equation in dissipative form of the Problem 3 for $z = 0.5$, $t = 1$, $h = 0.04$, $\triangle t = 0.01$.

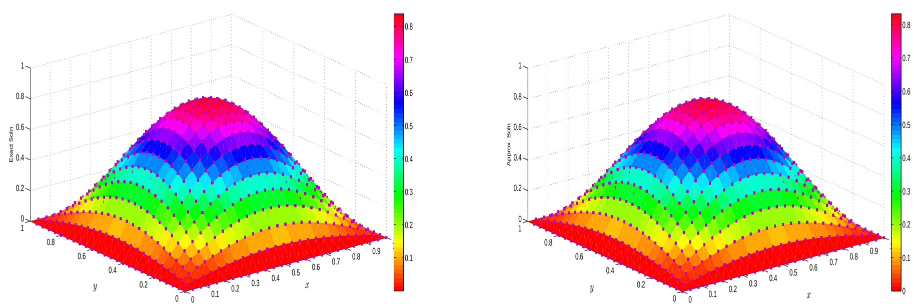

Fig. 9: The surface plot of the exact solution (left panel) and of the numerical solution (right panel) of the three-dimensional nonlinear wave equation in dissipative form of the Problem 3 for $z = 0.5$, $t = 1$, $h = 0.04$, $\triangle t = 0.01$.

kinetic equations [34] that have been recently proposed for the modeling of complex systems.

References

[1] C. Bianca, F. Pappalardo and S. Motta, Computers & Mathematics with Applications 58, 579-588 (2009).

[2] C. Bianca and S. Motta, Computers & Mathematics with Applications 57, 831-840 (2009).

[3] G. Arora, R.C. Mittal and B.K. Singh, J. Engg. Sci. Tech. 9(3), 104-116 (2014) special issue on ICMTEA 2013 conference.

[4] R. K. Mohanty and V. Gopal, Appl. Math. Model. 37, 2802-2815 (2013).

[5] Z. Zhang, D. Li, Y. Cheng and K. Liew, Acta Mech. Sin. 28(3), 808-818 (2012).

[6] M. Dehghan, Math. Comput. Simul. 71, 16-30 (2006).

[7] V. Gopal, R.K. Mohanty and L. M. Saha, J. Egypt. Math. Society 22, 280-285 (2014).

[8] R. C. Mittal and R. Bhatia, Appl. Math. Comput. 220, 496-506 (2013).

[9] S. Singh and P. Lin, Appl. Math. Comput. 230, 629-638 (2014).

[10] R. K. Mohanty, K. George and M. K. Jain, Int. J. Comput. Math. 56, 185-98 (1995).

[11] R. K. Mohanty, U. Arora and M. K. Jain, Appl. Math. Comput. 17, 277-289 (2001).
[12] R. K. Mohanty, M. K. Jain and U. Arora, Int. J. Comput. Math. 79, 133-142 (2002).
[13] R. K. Mohanty, Appl. Math. Comput. 162, 549-557 (2005).
[14] R. K. Mohanty, S. Singh and S. Singh, Appl. Math. Comput. 232, 529-541 (2014).
[15] V. A. Titarev and E. F. Toro, J. Comput. Phy. 204, 715-736 (2005).
[16] E. Shivanian, Engg. Analysis with Boundary Elements 50, 249-257 (2015).
[17] R. Bellman, B.G. Kashef and J. Casti, J Comput Phy 10, 40-52 (1972).
[18] R. Bellman, B. Kashef and E. S. Lee, R. Vasudevan, Pergamon, Oxford 371–376 (1976).
[19] J.R. Quan and C.T. Chang, Comput Chem Eng 13, 779-788 (1989).
[20] J.R. Quan and C.T. Chang, Comput Chem Eng 13, 1017-1024 (1989).
[21] C. Shu, Differential Quadrature and its Application in Engineering, Athenaeum Press Ltd., Great Britain, 2000.
[22] A. Korkmaz and İ. Dağ, Eng. Comput. Int. J. Comput. Aided Eng. Software 30(3), 320-344 (2013).
[23] C. Shu C and Y. T. Chew, Commun. Numer. Methods Eng. 13(8), 643-653 (1997).
[24] C. Shu and H. Xue, J. Sound Vib. 204(3), 549-555 (1997).
[25] C. Shu and B. E. Richards, Int J Numer Meth Fluids 15, 791-798 (1992).
[26] G. Arora and B. K. Singh, Appl. Math Comput 224, 166-177 (2013).
[27] R. Jiwari and J. Yuan, J. Math. Chem. 52(6), 1535-1551 (2014).
[28] J. R. Spiteri and S. J. Ruuth, SIAM Journal Numer Anal 40(2), 469-491 (2002).
[29] S. Gottlieb, D.I. Ketcheson and C. W. Shu, J. Sci. Comput. 38, 251-289 (2009).
[30] B. K. Singh, G. Arora and M. K. Singh, J. Egyp. Math. Society (2016), http://dx.doi.org/10.1016/j.joems.2015.11.003.
[31] B.K. Singh and G. Arora, Math. Eng. Sci. Aero. MESA 5 (2), 153-164 (2014).
[32] W. Lee, Tridiagonal matrices: Thomas algorithm, http://www3.ul.ie/wlee/ms6021_thomas.pdf, Scientific Computation, University of Limerick.
[33] C. Bianca, C. Dogbe, Communications in Nonlinear Science and Numerical Simulation 29, 240-256 (2015).
[34] C. Bianca, C. Dogbe, Nonlinearity 27, 2771-2803 (2014).

Brajesh K. Singh received the Master of Science degree in Mathematics in 2005 from CSJM University Kanpur. He received the Ph. D. degree in Mathematics from Indian Institute of Technology Roorkee in 2012. Currently, he is an Assistant Professor in Babasaheb Bhimarao Ambedkar University, Lucknow INDIA. His research interests are in the areas of applied mathematics including numerical analysis, mathematical simulation and cryptology. He has published research papers in reputed international journals of mathematical and engineering sciences. He is referee of various mathematical journals.

Carlo Bianca received the PhD degree in Mathematics for Engineering Science at Polytechnic University of Turin. His research interests are in the areas of applied mathematics and in particular in mathematical physics including the mathematical methods and models for complex systems, mathematical billiards, chaos, anomalous transport in microporous media and numerical methods for kinetic equations. He has published research articles in reputed international journals of mathematical and engineering sciences. He is referee and editor of mathematical journals. He is editor in chief of the Journal of Mathematics and Statistics.